Available online at www.sciencedirect.com
SCIENCE DIRECT
Spectrochimica Acta Part A 63 (2006) 174–181
SPECTROCHIMICA ACTA PART A
www.elsevier.com/locate/saa

Structural and spectral perspectives of a novel thiosemicarbazone synthesized from di-2-pyridyl ketone and 4-phenyl-3-thiosemicarbazide

V. Suni [a], M.R. Prathapachandra Kurup [a,*], Munirathinam Nethaji [b]

[a] *Department of Applied Chemistry, Cochin University of Science and Technology, Kochi 682022, Kerala, India*
[b] *Department of Inorganic and Physical Chemistry, Indian Institute of Science, Bangalore 560012, India*

Received 18 January 2005; received in revised form 30 April 2005; accepted 2 May 2005

Abstract

A new thiosemicarbazone, HL is synthesized from di-2-pyridyl ketone and 4-phenyl-3-thiosemicarbazide and structurally and spectrochemically characterized. ^{1}H NMR, ^{13}C NMR, COSY, HMQC and IR spectra of the compound are studied and the proton magnetic resonance spectrum reveals some unprecedented observations. The thione form is predominant in the solid state, as supported by the crystal structure and IR data, while a thiol–thione equilibrium is proposed in the solution state by NMR studies. The compound crystallizes into a monoclinic lattice with space group *C*2/*c* and the *ZE* conformation is exhibited by the thiosemicarbazone. Intra- and intermolecular hydrogen-bonding interactions give rise to a two-dimensional packing in the crystal lattice.

Keywords: Di-2-pyridyl ketone; Thiosemicarbazone; HMQC; COSY; Crystal structure

1. Introduction

For the past three decades, thiosemicarbazones with the general formula (R^1)NH–C(S)–NH–N(R^2R^3) has remained an important ligand construction unit in both the neutral and anionic forms [1–13]. These organic molecules with potential donor atoms in their structural skeleton fascinate coordination chemists with their versatile chelating behavior. The coordinating ability of thiosemicarbazides to both transition and main group metallic cations is attributed to the extended delocalization of electron density over the –NH–C(S)–NH–N= system, which is enhanced by substitution at the N(4) position. Condensation of thiosemicarbazides with aromatic aldehydes or ketones extend the electron delocalization along the azomethine bond. Presence of additional donor sites in the ketonic part as in the case of di-2-pyridyl ketone, offer much more coordination possibilities for the thiosemicarbazone ligand.

Interestingly, di-2-pyridyl ketone (dpk), as such can function as a ligand construction unit, chelating with metal ions and forming promising clusters and cubanes with excellent ferromagnetic characteristics [14–16]. The hydrolysed derivative of dpk, commonly referred to as the gem-diol form of di-2-pyridyl ketone coordinate to metals either in the monoanionic or dianionic form, giving rise to infinite arrays. Hence, incorporation of di-2-pyridyl ketone into an N(4)-substituted thiosemicarbazone chain offer a variety of binding modes with possible extension into polymeric structures. However, the coordination chemistry of substituted or unsubstituted thiosemicarbazones of di-2-pyridyl ketone is quite unexplored with few previous reports [17–21]. This prompted our study into the synthesis and characterization of di-2-pyridyl ketone thiosemicarbazones and their metal complexes [22–24], and here we report the structural and spectral perspectives of a new compound,

* Corresponding author. Tel.: +91 484 2575804; fax: +91 484 2577595.
E-mail address: mrp@cusat.ac.in (M.R. Prathapachandra Kurup).

1386-1425/$ – see front matter © 2005 Elsevier B.V. All rights reserved.
doi:10.1016/j.saa.2005.05.001

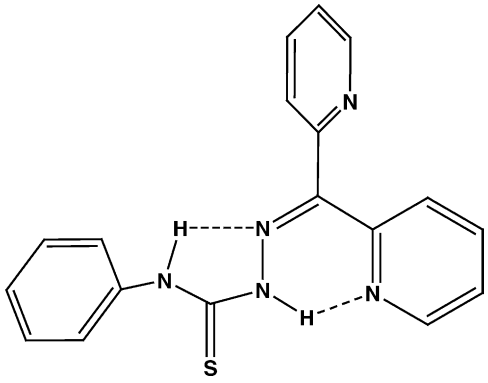

Fig. 1. Structure of compound HL.

di-2-pyridyl ketone *N*(4)-phenylthiosemicarbazone, HL (Fig. 1).

2. Experimental

2.1. Materials

Commercial reagents, phenyl isothiocyanate (Fluka), hydrazine hydrate (Lancaster) and di-2-pyridyl ketone (Aldrich) were used as received. Elemental analyses were carried out at CDRI, Lucknow, India, with Heraeus Elemental Analyser. Infrared spectra were recorded on ABB Bomem FTIR instrument using KBr pellets in the range of 4000–500 cm^{-1}. Electronic spectrum in the solid state was recorded on Ocean Optics, SD2000 Fibre Optic Spectrometer. The ^{1}H NMR, ^{13}C NMR, COSY and HMQC spectra were recorded using Bruker DRX 500, with $CDCl_3$ as solvent and TMS as standard at Sophisticated Instruments Facility, Indian Institute of Science, Bangalore, India.

2.2. Synthesis of HL

Preparation of compound HL was carried out as in Scheme 1, adapting a reported procedure [25]. A solution of phenyl isothiocyanate (0.675 g, 5 mmol) in 20 ml of ethanol was continuously stirred with an ethanolic solution of hydrazine hydrate (0.250 g, 5 mmol) for 1 h. The white product of *N*(4)-phenylthiosemicarbazide thus formed was washed, dried and recrystalized from ethanol. A ethanolic solution of *N*(4)-phenyl thiosemicarbazide (0.836 g, 5 mmol) was then refluxed with methanolic solution of di-2-pyridyl ketone (0.921 g, 5 mmol) continuously for 4 h after adding one drop of acetic acid. Light yellow crystals of the thiosemicarbazone were separated upon cooling, which were filtered and washed with methanol. The compound was recrystalized from ethanol and dried over P_4O_{10} in vacuo.

Table 1
Crystal data and structural refinement for HL

Parameters	HL
Empirical formula	$C_{18}H_{15}N_5S$
Formula weight, *M*	333.41
Crystal system	Monoclinic
Space group	*C*2/*c*
Lattice constants	
a (Å)	22.073(19)
b (Å)	9.740(8)
c (Å)	16.380(14)
α (°)	90.00
β (°)	104.766(13)
γ (°)	90.00(9)
Volume *V* ($Å^3$)	3405(5)
Z	8
Calculated density, ρ ($Mg\ m^{-3}$)	1.301
Absorption coefficient, μ (mm^{-1})	0.199
F(0 0 0)	1392
Crystal size (mm)	0.80 × 0.64 × 0.61
θ Range for data collection	1.91–27.32
Limiting indices	$-28 \le h \le 25$, $-11 \le k \le 12$, $-20 \le l \le 20$
Reflections collected	12701
Unique reflections	3534 [R_{int} = 0.0184]
Completeness to θ	27.32 (91.8%)
Absorption correction	None
Refinement method	Full-matrix least-squares on F^2
Data/restraints/parameters	3534/0/278
Goodness-of-fit on F^2	1.057
Final *R* indices [$I > 2\sigma(I)$]	R_1 = 0.0521, wR_2 = 0.1525
R indices (all data)	R_1 = 0.0599, wR_2 = 0.1621
Largest difference peak and hole (e $Å^{-3}$)	0.814 and −0.234

2.3. X ray data collection, structure solution and refinement

The crystallographic data and structure refinement parameters of compound HL are given in Table 1. A light yellow rectangular single crystal of HL with approximate dimensions 0.08 mm × 0.64 mm × 0.61 mm was used for data collection. Measurement of X-ray diffraction data was done at 293(2) K using Mo Kα radiation of wavelength 0.71073 Å with Bruker SMART APEX CCD diffractometer equipped

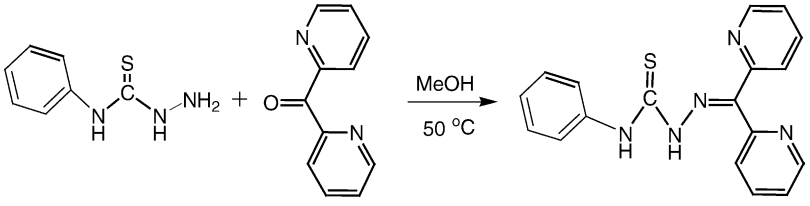

Scheme 1.

with a fine focus sealed tube X-ray source. The structure was solved by direct methods and refined by least-square on F_0^2 using SHELXL-97 [26]. Refinement of F^2 was done against all reflections. All *esd*s, except the *esd* in the dihedral angle between two least square planes, are estimated using the full covariance matrix. The SMART software was used for data acquisition and the SAINT software for data extraction [27]. The graphics tool was DIAMOND [28]. All non-hydrogen atoms were refined anisotropically, while the hydrogen atoms were treated with a mixture of independent and constrained refinement and used for structure factor calculation only.

3. Results and discussion

3.1. Synthesis of HL

The compound is obtained as crystalline product from the condensation of di-2-pyridyl ketone with 4-phenyl-3-thiosemicarbazone and the single crystals suitable for X-ray analysis were grown by slow evaporation of a dilute solution in methanol. Elemental analyses, found (calcd.): C 64.79(64.84); H 4.53(4.46); N 21.11(21.01), mp 135 °C, yield 62%.

3.2. ^{1}H NMR

Proton magnetic resonance spectroscopy is a helpful tool for the identification of organic compounds in conjunction with other spectrometric informations. The ^{1}H NMR spectrum of the compound along with the spectral assignments is given in Fig. 2. A sharp singlet, which integrates as one hydrogen at $\delta = 14.55$ ppm is assigned to the proton attached to the nitrogen atom N(4), while another similar singlet at $\delta = 9.55$ ppm is assigned to the N(5)H proton. The downfield shifts of these protons are assigned to their hydrogen-bonding interactions with adjacent nitrogen atoms N(1) and N(3). Hydrogen-bonding decreases the electron density around the proton, and thus moves the proton absorption to a lower field [29]. Absence of any coupling interactions by N(4)H and N(5)H protons due to the lack of availability of protons on neighboring atoms render singlet peaks for the imine protons. Two doublets at $\delta = 8.84$ and 8.675 ppm are assigned to the C(1)H and C(11)H protons, respectively. These signals are shifted to lower field due to electronic effect of the adjacent electronegative pyridyl nitrogens and the more downfield shift of C(1)H can be attributed to the increased charge density on N(1) resulted by its hydrogen-bonding to N(4)H. Coupling of these protons with the C(2) and C(10) protons splits their signals into doublets. The proton resonances of the two pyridyl rings also appear separately in the NMR spectrum, due to the intramolecular hydrogen-bonding. There are two multiplets at $\delta = 7.815$ and 7.855 ppm corresponding to similar protons on C(3) and C(9) of the two pyridyl rings, while the C(2)H and C(10)H resonances appear overlapped in the multiplet at $\delta = 7.40$ ppm. A doublet at $\delta = 7.57$ ppm ideally correspond to C(4)H and C(8)H protons. However, the C(4)H protons are found to have experienced a greater downfield shift into the multiplet at $\delta = 7.815$, as evident from the HMQC spectrum. The resonances for the C_6H_5– group appear as a doublet at δ 7.705 ppm (ortho), and as multiplets at δ 7.40 and 7.24 ppm corresponding to meta and para phenyl protons. All the assignments made above are observed to be in general agreement with previous reports on di-2-pyridyl ketone thiosemicarbazones [16,17]. However, interestingly, the ^{1}H NMR spectrum of the present compound reveals some more singlet peaks in the higher field region beyond $\delta = 2.2$ ppm. A comparatively weak signal at $\delta = 2.18$ ppm together with a sharp peak at $\delta = 1.60$ ppm can be assigned to an –SH peak attributable to the possible presence of the thiol tautomer in solution. Thiosemicarbazones are believed to exhibit a thione–thiol equilibrium in the solution state. However, in all the previous reports mentioned

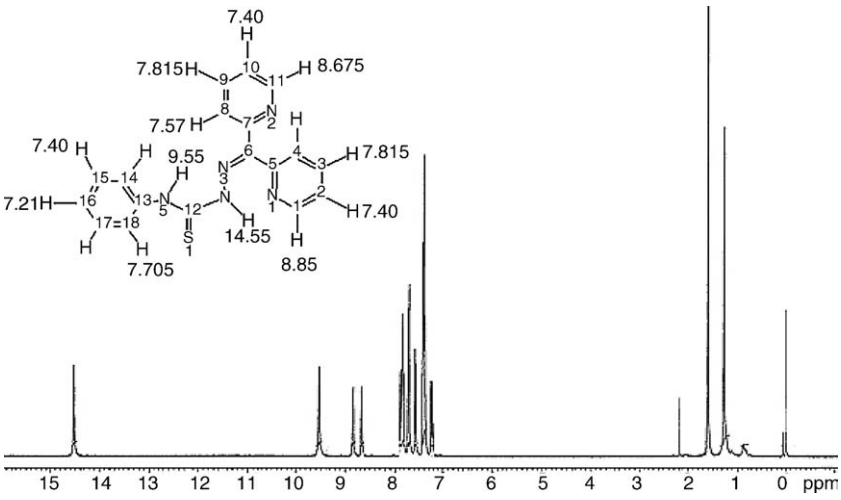

Fig. 2. ^{1}H NMR spectrum.

above, such an –SH signal was absent and the compounds were established to retain their structure in solution. Another interesting singlet at δ 1.25 ppm, which integrates as two protons, is typical of the present compound and it is assigned to be of the protons on the hetero atoms N(4) and N(5), which are subjected to hydrogen-bonding in $CdCl_3$ solvent [29]. To the best of our knowledge, such a typical evidence for the intramolecular hydrogen-bonding in N(4)-substituted thiosemicarbazones has never been previously obtained from the ^{1}H NMR spectrum.

3.3. ^{13}C NMR

The ^{13}C NMR spectrum provides direct information about the carbon skeleton of the molecule. Assignment of different resonant peaks to respective carbon atoms are presented in Fig. 3. Considering the two pyridyl rings non-equivalent, resulting from the hydrogen-bonding interaction, there are 16 unique carbon atoms in the molecule, which give a total of 16 different peaks in the ^{13}C NMR spectrum. In both the pyridyl rings, the C(1) and C(11) carbon atoms adjacent to the more electronegative nitrogen atoms N(1) and N(2) are shifted further downfield when compared to the neighboring carbon atoms. Also, the carbon atoms at para position to the hetero atoms, viz. C(3) and C(9) resonate at lower field values when compared to the meta positioned carbons, C(2), C(4), C(8) and C(10). However, the non-protonated carbons C(5) and C(7) are showing more downfield shift in the pyridyl rings due to an increased electron density resulting from the presence of electronegative nitrogen atom and π electron delocalization in the magnetic environment. Hence, the ^{13}C peaks of the two pyridyl rings are assigned as follows: C(1), 148.932 ppm; C(2), 124.429 ppm; C(3), 137.684 ppm; C(4), 125.017 ppm; C(5), 155.033 ppm; C(7), 156.671 ppm; C(8), 127.510 ppm; C(9), 137.804 ppm; C(10), 124.721 ppm; C(11), 149.557 ppm. The non-protonated carbon atom at C(6) is shifted farthest downfield in the spectrum (δ 177.422 ppm), effected by the magnetic interaction of two bulky pyridyl rings and the π electron delocalization on the C(6) = N(3) bond. Similarly, the C(12) carbon atom resonance is also observed at a lower field of 152.349 ppm, resultant of the conjugative effect of the –N(3)–N(4)–C(S)–N(5)– thiosemicarbazone skeleton. The three different types of aromatic carbons on the substituted phenyl ring are clearly distinguishable in the ^{13}C NMR spectrum. The peak corresponding to the para positioned carbon atom C(16) is observed rather upfield when compared to its ortho [C(14) and C(18)] and meta [C(15) and C(17)] counterparts. The phenyl resonances are: C(14) and C(18), 124.819 ppm; C(15) and C(17), 129.449 ppm; C(16), 126.691 ppm.

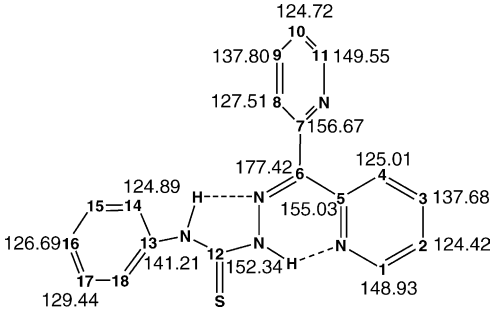

Fig. 3. ^{13}C NMR assignments of HL.

3.4. ^{1}H–^{1}H COSY

The COSY spectrum reveals the ^{1}H–^{1}H coupling interactions in a molecule. It is usually plotted as three-dimensional contours, where the conventional spectrum is represented along the diagonal (Fig. 4). The cross-peaks along both the sides of the diagonal identify the nuclei that are coupled to each other. On the contrary, the protons that are decoupled from the adjacent ones due to the lack of α-protons will show no correlation in the spectrum. For instance, in the COSY spectrum of the present compound, absence of any off-diagonal peaks extending from δ = 14.55 and 9.55 ppm confirm their assignment to N(4)H and N(5)H protons, respectively. However, extending horizontal and vertical lines from δ = 8.84 ppm [C(1)H] and 8.675 ppm [C(11)H] encounter cross-peaks at δ 7.40 ppm, where the C(2)H and C(10)H resonances are merged into multiplets along with the phenyl ring proton resonances. The comparatively weaker coupling interactions of C(1)H and C(11)H with the β-positioned C(3)H and C(9)H protons are shown by the poorly resolved cross peaks at δ 7.815 and 7.855 ppm. This also helps to accurately assign C(3)H (δ 7.815 ppm) and C(9)H (δ 7.855 ppm) protons to their respective values, which is contrary to the expected more downfield shift of C(3)H proton of the hydrogen bonded pyridine ring. COSY spectrum also turns out very helpful in the accurate assignment of proton resonances in the aromatic region. The multiplets of the C(3)H and C(9)H protons show coupling interactions with the doublet at δ 7.57 ppm [C(4)H and C(8)H] and with the multiplet at δ 7.40 ppm [C(2)H and C(10)H]. However, the C(3) and C(9) protons show no

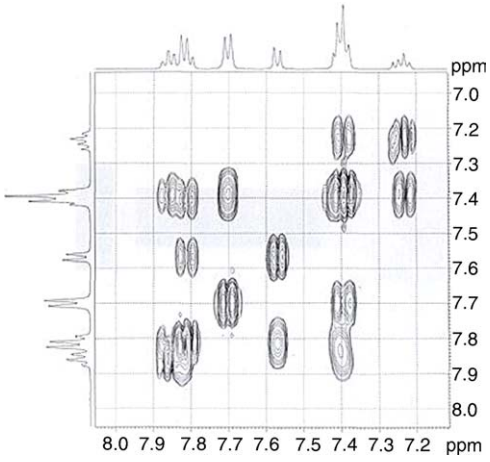

Fig. 4. ^{1}H–^{1}H COSY spectrum.

interactions with the doublet at δ 7.705 ppm, which helps to assign the latter peak to the phenyl protons at the ortho position, i.e., C(14)H and C(18)H. Coupling interactions of these protons are observed at δ 7.40 ppm, thus assigning the multiplet to the meta positioned phenyl protons C(15)H and C(17)H also. Assignment of the multiplet at δ 7.24 ppm to the para phenyl proton C(16)H is clearly evident from the COSY, as its only correlation is observed with the multiplet at δ 7.40 ppm, which is assigned to the neighboring C(15)H and C(17)H.

3.5. ^{1}H–^{13}C HMQC

The ^{1}H–^{13}C heteronuclear multiple-quantum coherence (HMQC) spectrum provides information regarding the interactions between the protons and the carbon atoms to which they are directly attached. Contrary to COSY spectrum, only the resultant interactions are plotted as contour peaks in the HMQC spectrum (Fig. 5). In the present compound, the absence of any contours at δ = 155.033, 177.422, 156.671, 152.349 and 141.217 ppm assign them to the C(5), C(6), C(7), C(12) and C(13) carbon atoms, respectively. This is because, they belong to the non-protonated carbon atoms on the pyridyl rings, C(6)=N(3); C(12)=S(1) and on the phenyl ring, respectively, all of which are unable to show any direct ^{1}H–^{13}C coupling interactions. The peaks observed at δ 148.932 and 149.557 ppm are assigned to C(1) and C(11) carbon atoms, respectively, due to their interactions with ^{1}H resonances at δ 8.84 and 8.675 ppm. The evidence for the presence of protons attached to three different types of carbon atoms in the multiplets at δ 7.855 and 7.815 ppm is obtained from the ^{13}C–^{1}H HMQC spectrum, which gives three contours at ^{13}C signals δ 137.684 ppm [C(3)]; 137.804 ppm [C(9)] and 124.429 ppm [C(4)]. The doublets at δ 7.705 and 7.57 ppm and the quartet at δ 7.24 ppm show contours at δ 124.81 ppm [C(14) and C(18)], 127.510 ppm [C(8)] and 126.691 ppm [C(16)], which help to distinguish these ^{13}C resonances, which are close to each other. The multiplet at δ 7.40 ppm in the ^{1}H NMR shows two different resultant contour peaks around δ 124 and 129 ppm, which reveal the presence of both the phenyl and pyridyl ring proton resonances in the multiplet. With the help of these contours, the carbon atoms at meta positions of the phenyl ring are assigned to the ^{13}C resonance at δ 129.449 ppm, while the carbon atoms at meta positions to the nitrogen atoms on the two pyridyl rings are assigned at δ 124.721 and 124.429 ppm.

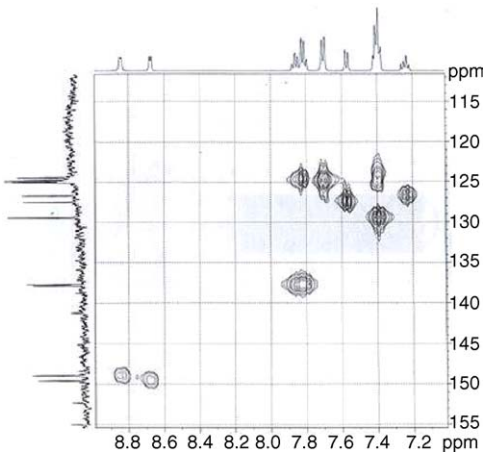

Fig. 5. ^{1}H–^{13}C HMQC spectrum of HL.

3.6. IR spectrum of HL

The thioamide function in the thiosemicarbazone skeleton usually exhibit free –NH stretching vibrations as multiple bands near 3300–3060 cm^{-1}. Multiple bands usually result from the association of thioamide groups in different molecules to form dimers or polymers [29]. However, the samples in the solid state can give rise to a widened band near 3400 cm^{-1}, as in the case of the present compound, HL. Absence of any bands at in the 2800–2550 cm^{-1} region points towards the lack of –SH stretching absorptions in the molecule. It reveals the presence of only the thione tautomer in the solid state. The azomethine stretching vibrations, characteristic of a Schiff base, are observed at 1592 cm^{-1} [30]. The band at 1529 cm^{-1} is the resultant of the interactions between N–H bending and C–N stretching vibrations of the C–N–H group of the thioamide function. A weak band at 1253 cm^{-1} also results from the N–H bending and C–N stretching interactions. The thiocarbonyl group shows absorptions at 1320 and 806 cm^{-1}, while additional bands in the broad region of 1400–700 cm^{-1} are due to vibrations involving interactions between C=S stretching and C–N stretching of the C=S group attached to a nitrogen atom. The bands at 1174 and 1110 cm^{-1} correspond to the in-plane vibrations of the pyridyl ring, while the out-of-plane vibrations are observed at 762 and 695 cm^{-1}.

3.7. UV–visible spectrum of HL

In contrast to the infrared spectrum, the electronic spectrum is not used primarily for the identification of individual functional groups, but rather to show the relationship between functional groups, chiefly conjugation [31]. The UV–visible spectra of organic compounds are associated with the electronic transitions between energy levels, and at wavelengths above 200 nm, excitation of electrons from the π-orbitals usually occurs giving rise to informative spectra [32]. Solid-state reflectance spectrum of the present thiosemicarbazone reveals the spectral bands in close proximity with similar systems reported earlier (Fig. 6). The $\pi \rightarrow \pi^*$ transitions of the pyridyl ring and the thiosemicarbazone imine function are rather weak, observed at ca. 35300 cm^{-1}. However, an intense band at ca. 27900 cm^{-1} is attributed to the $\pi \rightarrow \pi^*$ transition of the C=S group and the $n \rightarrow \pi^*$ transition of the pyridine ring [29].

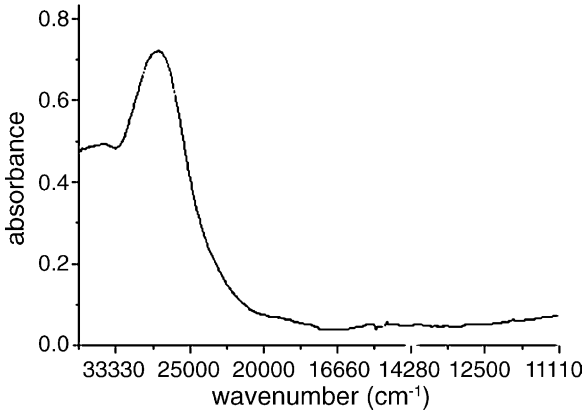

Fig. 6. Electronic spectrum of HL.

3.8. Crystal structure

The molecular structure of HL along with atomic numbering scheme is given in Fig. 7 and selected bond lengths and angles are given in Table 1. The compound crystallizes into a monoclinic lattice with space group *C*2/*c*. The molecule exists in the *ZE* conformation of thiosemicarbazones since *Z* and *E* configurations are perceived with respect to C6–N3 and C12–N4 bonds, respectively. A torsion angle value of 171.58(5)° corresponding to the S1–C12–N4–N3 moiety confirms the trans configuration of the thiocarbonyl S1 atom [33]. The thiosemicarbazone skeleton comprising of atoms N3, N4, C12, S1 and N5 is almost planar with a maximum deviation of −0.0650(4) Å from the mean plane. The C6–N3 bond distance (1.2858(8) Å) is appreciably close to that of a C=N double bond (1.28 Å) [34], confirming the azomethine bond formation. The existence of the thiosemicarbazone in the thione form in the solid state is evidenced by the C(12)–S(1) bond distance of 1.6763(12) Å, which is very close to a formal C=S bond length (1.60 Å) [35]. However, the N(3)–N(4) (1.3573(10)) and N(4)–C(12) (1.3616(9)) bond distances are observed intermediate between the ideal values of corresponding single [N–N; 1.45 Å and C–N; 1.47 Å] and double bonds [N=N; 1.25 Å and C=N; 1.28 Å] [36], which is in support of an extended π delocalization along the thiosemicarbazone chain. Among the three aromatic rings, the pyridyl ring Cg(1) with the N(1) nitrogen on it, suffers least deviation from the thiosemicarbazone moiety at a dihedral angle of 17.65(1)° between the two corresponding planes. The pyridyl ring Cg(2) and the phenyl ring Cg(3) make a dihedral angle of 60.81(2)° between each other and they are deviated from the central thiosemicarbazone moiety at angles 35.98(1)° and 57.34(2)°, respectively. The largest deviation is observed between the planes of the two pyridyl rings positioned at a dihedral angle of 67.66(2) between each other, which owes mainly to the steric interactions of the bulky pyridyl groups. Two prominent intramolecular hydrogen-bonding interactions, viz. N(4)–H(4)N···N(1) and N(5)–H(5)N···N(3) lead to the formation of one six-membered ring and one five-membered ring comprising of atoms N(1), C(5), C(6), N(3), N(4), H(4)N and N(3), N(4), C(12), N(5), H(5)N, respectively. A short interatomic contact, C(8)–H(8)···N(2), at a C(8)–N(3) distance of 2.919(2) Å also helps to stabilize the present conformation of the thiosemicarbazone Table 2.

Table 2
Selected bond lengths (Å) and bond angles (°) of HL

	HL
C(6)–N(3)	1.2858(8)
N(3)–N(4)	1.3573(10)
N(4)–C(12)	1.3616(9)
C(12)–S(1)	1.6763(12)
N(3)–N(4)	1.3573(10)
C(12)–N(5)	1.3392(8)
N(5)–C(13)	1.4137(10)
C(6)–C(7)	1.4935(12)
C(5)–C(6)	1.4806(9)
C(7)–C(6)–C(5)	118.88(4)
C(5)–C(6)–N(3)	127.81(6)
C(6)–N(3)–N(4)	120.51(5)
N(3)–N(4)–C(12)	120.03(4)
N(4)–C(12)–S(1)	117.44(4)
N(4)–C(12)–N(5)	114.27(6)
C(12)–N(5)–C(13)	128.50(6)

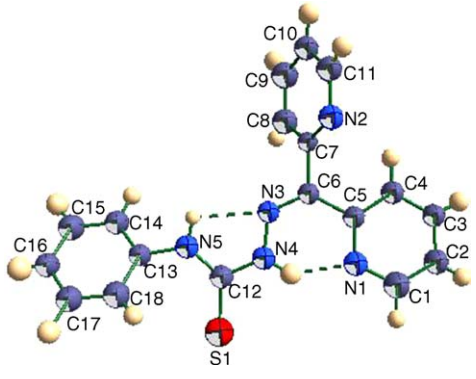

Fig. 7. Molecular structure of HL. Displacement ellipsoids are drawn at 50% probability level.

The packing of the molecules of HL is shown in Fig. 8, where the unit cell is viewed down the '*c*' axis. The basic unit of the crystal packing consists of a set of two molecules which are held together by intermolecular hydrogen-bonding interactions involving N(2) (acceptor) of one molecule and N(5) (donor) of the adjacent molecule through H(5)N. Two adjacent sets are then aligned in an offset fashion, which forms the repeating unit of the packing in the crystal lattice. It is interesting to note that no intermolecular interactions are perceived between these adjacent sets and the overall packing in a two-dimensional manner is affected by the offset alignment of neighboring sets in the unit cell. Some weak C–H···π and π–π interactions, viz. C(15)–H(15)···[1]···Cg(1)^{i} [Cg(1): N(1), C(1), C(2), C(3), C(4), C(5); $d_{C(15)\cdots Cg}$ = 3.5800 Å; i = −*x*, 2 − *y*, 1 − *z*] and Cg(2)···[1]···Cg(2)^{ii}; [Cg(2): N(2), C(7), C(8), C(9), C(10), C(11); $d_{Cg\cdots Cg}$ = 3.5809 Å; ii = −*x*, *y*, 1/2 − *z*] are the shortest interactions observed of their

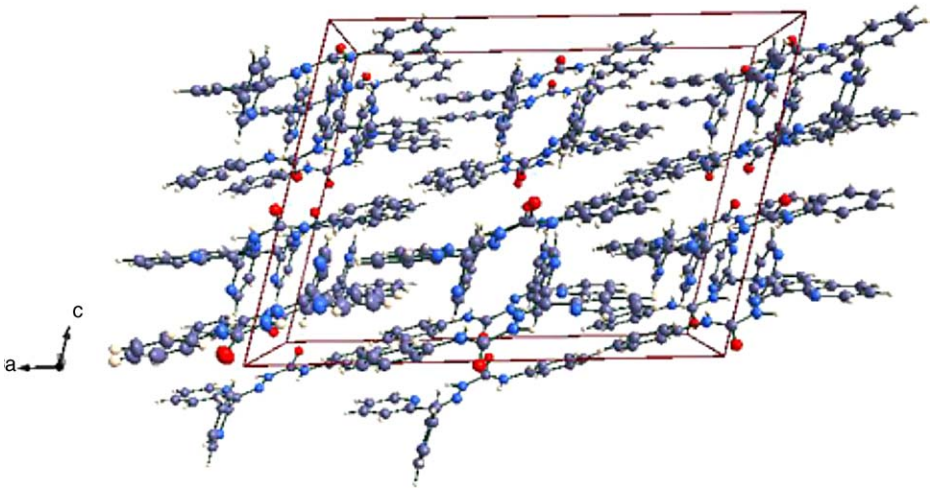

Fig. 8. Molecular packing diagram of HL, the unit cell is viewed down the '*b*' axis.

type in the lattice of the present compound. However, the two intra-molecular hydrogen-bonding interactions observed are much effective, operating at appreciably short distances, viz. N(5)–H(5)N···N(3)^{iii} [$d_{D\cdots A}$ = 2.596(2) Å; iii = *x*, *y*, *z*] and N(4)–H(4)N···N(1)^{iii} [$d_{D\cdots A}$ = 2.670(2) Å]. These intra-molecular hydrogen-bonding interactions have substantial effects upon the structural as well as spectral properties of the thiosemicarbazone.

Acknowledgements

The authors are thankful to Sophisticated Instruments Facility, IISc Bangalore, India, for NMR measurements. V. Suni acknowledges State Counsil for Science, Technology and Environment, Kerala, India, for financial support in the form of a fellowship.

Appendix A. Supplementary data

Crystallographic data for structural analysis has been deposited with the Cambridge Crystallographic Data center, CCDC 248281 for compound HL. Copies of this information maybe obtained free of charge from The Director, CCDC, 12 Union Road, Cambridge, CB2, IEZ, UK (fax: +44-1223-336-033; e-mail: deposit@ccdc.cam.ac.uk or http://www.ccdc.cam.ac.uk).

References

[1] A. Sreekanth, H.-K. Fun, M.R.P. Kurup, Inorg. Chem. Commun. 7 (2004) 1250.
[2] M. Joseph, V. Suni, M.R.P. Kurup, M. Nethaji, A. Kishore, S.G. Bhat, Polyhedron 23 (2004) 3069.
[3] M. Joseph, V. Suni, C.R. Nayar, M.R.P. Kurup, H.-K. Fun, J. Mol. Struct. 705 (2004) 63.
[4] A. Sreekanth, M.R.P. Kurup, Polyhedron 22 (2003) 3321.
[5] H. Beraldo, W.F. Nacif, L.R. Teixeira, J.S. Reboucas, Transition Met. Chem. 27 (2002) 85.
[6] J.S. Casas, A. Castineiras, M.C. Rodriguez-Arguelles, A. Sanchez, J. Sordo, A. Vazquez-Lopez, E.M. Vazquez-Lopez, J. Chem. Soc., Dalton Trans. (2000) 2267.
[7] P. Bindu, M.R.P. Kurup, T.R. Satyakeerthy, Polyhedron 18 (1999) 321.
[8] B.S. Garg, M.R.P. Kurup, S.K. Jain, Y.K. Bhoon, Synth. React. Inorg. Met. Org. Chem. 28 (1998) 1415.
[9] J.R. Dilworth, J.S. Lewis, J.R. Miller, Y. Zheng, J. Chem. Soc., Dalton Trans. (1995) 1357.
[10] B.S. Garg, M.R.P. Kurup, S.K. Jain, Y.K. Bhoon, Transition Met. Chem. 16 (1991) 111.
[11] B.S. Garg, M.R.P. Kurup, S.K. Jain, Y.K. Bhoon, Transition Met. Chem. 13 (1988) 247.
[12] D.L. Klayman, J.P. Scovill, J.F. Bartosevich, J. Bruce, J. Med. Chem. 26 (1983) 39.
[13] D.H. Petering, Bioinorg. Chem. 1 (1972) 255.
[14] M.L. Tong, S.L. Zheng, J.X. Shi, Y.X. Tong, H.K. Lee, X.M. Chen, J. Chem. Soc., Dalton Trans. (2002) 1727.
[15] Z.E. Serna, M.K. Urtiaga, M.G. Barandika, R. Cortes, S. Martin, L. Lezama, M.I. Arriortua, T. Rojo, Inorg. Chem. 40 (2001) 4550.
[16] S.R. Breeze, S. Wang, J.E. Greedan, N.P. Raju, Inorg. Chem. 35 (1996) 6945.
[17] J.K. Swearingen, W. Kaminsky, D.X. West, Transition Met. Chem. 27 (2002) 724.
[18] J.K. Swearingen, D.X. West, Transition Met. Chem. 26 (2001) 252.
[19] C. Duan, X. You, T.C. Mak, Acta Crystallogr. C 54 (1998) 1395.
[20] M. Maji, M. Chatterjee, S. Ghosh, S.K. Chattopadhyay, B.M. Wu, T.C.W. Mak, J. Chem. Soc., Dalton Trans. (1999) 135.
[21] C. Duan, B. Wu, T.C. Mak, J. Chem. Soc., Dalton Trans. (1996) 3485.
[22] V. Philip, V. Suni, M.R.P. Kurup, Acta Crystallogr. C 60 (2004) o856.
[23] V. Philip, V. Suni, M.R.P. Kurup, M. Nethaji, Polyhedron 23 (2004) 1225.
[24] A. Usman, I.A. Razak, S. Chantrapromma, H.K. Fun, V. Philip, A. Sreekanth, M.R.P. Kurup, Acta Crystallogr. C 58 (2002) o652.
[25] D.L. Klayman, J.F. Bartosevich, T.S. Griffin, C.J. Mason, J.P. Scovill, J. Med. Chem. 22 (1979) 855.
[26] G.M. Sheldrick, SHELXTL Version 5.1, Software Reference Manual, Bruker AXS Inc., Madison, WI, USA, 1997.

[27] Siemens, SMART and SAINT, Area Detector Control and Integration Software, Siemens Analytical X-ray Instruments Inc., Madison, WI, USA, 1996.
[28] K. Brandenburg, H. Putz, DIAMOND Version 3.0, Crystal Impact, GbR, Postfach 1251, D-53002 Bonn, Germany, 2004.
[29] R.M. Silverstein, G.C. Bassler, T.C. Morrill, Spectrometric Identification of Organic Compounds, fourth ed., John Wiley & Sons, New York, 1981.
[30] W. Kemp, Organic Spectroscopy, third ed., Macmillan, Hampshire, 1996.
[31] R.T. Morrison, R.N. Boyd, Organic Chemistry, fourth ed., Allyn and Bacon Inc., London, 1990.
[32] D.H. Williams, I. Fleming, Spectroscopic Methods in Organic Chemistry, fourth ed., McGraw-Hill, London, 1989.
[33] D. Chattopadhyay, T. Banerjee, S.K. Mazumdar, S. Ghosh, R. Kuroda, Acta Crystallogr. C 43 (1987) 974.
[34] J. March, Advanced Organic Chemistry, Reactions, Mechanisms and Structure, fourth ed., Wiley, New York, 1992.
[35] J.E. Huheey, E.A. Keiter, R.L. Keiter, Inorganic Chemistry, Principles of Structure and Reactivity, fourth ed., Harper Collins College Publishers, New York, 1993.
[36] G.J. Palenik, D.F. Rendle, W.S. Carter, Acta Crystallogr. B 30 (1974) 2390.